Available online at www.sciencedirect.com

ScienceDirect

Publishing Services by Elsevier

International Journal of Naval Architecture and Ocean Engineering 8 (2016) 577–588

http://www.journals.elsevier.com/international-journal-of-naval-architecture-and-ocean-engineering/

Engineering criticality analysis on an offshore structure using the first- and second-order reliability method

Beom-Jun Kang, Jeong-Hwan Kim, Yooil Kim*

Department of Naval Architecture and Ocean Engineering, INHA University, 100, Inha-Ro, Nam-Gu, Incheon, South Korea

Received 15 March 2016; revised 3 May 2016; accepted 11 May 2016
Available online 30 July 2016

Abstract

Due to the uncertainties related to the flaw assessment parameters, such as flaw size, fracture toughness, loading spectrum and so on, the probability concept is preferred over deterministic one in flaw assessment. In this study, efforts have been made to develop the reliability based flaw assessment procedure which combines the flaw assessment procedure of BS7910 and first- and second-order reliability methods (FORM/SORM). Both crack length and depth of semi-elliptical surface crack at weld toe were handled as random variable whose probability distribution was defined as Gaussian with certain means and standard deviations. Then the limit state functions from static rupture and fatigue perspective were estimated using FORM and SORM in joint probability space of crack depth and length. The validity of predicted limit state functions were checked by comparing it with those obtained by Monte Carlo simulation. It was confirmed that the developed methodology worked perfectly in predicting the limit state functions without time-consuming Monte Carlo simulation.

Keywords: Engineering criticality analysis; BS7910; Fracture mechanics; Crack propagation; Limit state function; FORM; SORM

1. Introduction

Welded structures are inevitably susceptible to the cracks either at weld toe or within welds due to the variety of reasons, such as excessive residual stress, inclusion of impurities and unexpected lack of fusion and so on. These cracks pose a major threat to the integrity of entire structure during it service life under environmental loadings acting on it such as wind, wave and current loads. Engineering criticality analysis, which targets to assess the fitness for service of the structure during its lifetime, is defined as a fracture mechanics based numerical analysis aiming at the assessment of flaw susceptibility under the loadings that the structure is exposed to. A flaw may fracture, either in brittle or ductile way, due to excessive loading or may grow to the critical size which may lead to successive fracture or functional degradation such as leak. Flaw assessment is critical to both fabricator and operator point of view because a decision needs to be made whether the existing flaw should be repaired or not, which has a huge impact in terms of the CAPEX and OPEX.

Flaw assessment procedure is well documented in BS7910 (BSI, 2005) or other equivalent standards such as API (API, 2007). Even though the analysis procedure is fully mature, it lacks the consideration of the probabilistic natures of the analysis parameters such as crack length, depth, fracture toughness, crack growth constants and loading parameters etc. All these parameters are difficult to define in deterministic way due to the complexities involved in, hence the standards take this random effect into account by either relying on partial safety factor or using statistically conservative values, such as mean minus two standard deviation or something equivalent. On the other hand, the reliability concept has been utilized in many engineering field for years targeting the

* Corresponding author. Fax: +82 32 864 5850.
E-mail addresses: kjoon86@hanmail.net (B.-J. Kang), jhk81@inha.edu (J.-H. Kim), yooilkim@inha.ac.kr (Y. Kim).
Peer review under responsibility of Society of Naval Architects of Korea.

http://dx.doi.org/10.1016/j.ijnaoe.2016.05.014

probability based assessment on the structural integrity. The probabilistic nature of analysis parameters may be handled by a Monte Carlo simulation (Metropolis and Ulam, 1949), but large number of sample and corresponding simulation require practically infeasible computational burden. The computation cost increase dramatically especially when the number of random variables exceed 3 or 4 eventually leading to several thousand calculations. To overcome this difficulty, so called first- and second-order reliability concept was developed and successfully applied in many engineering structural problems (Cornell, 1969; Hasofer et al., 1974; Rackwitz and Fiessler, 1978; Fiessler et al., 1979; Breitung, 1984; Hohenbichler et al., 1987; Tvedt, 1990). First- and second order reliability methods rely on Taylor series expansion in joint probability space to approximate the Limit State Function (LSF) with some truncation errors. First Order Reliability Method (FORM) approximate the limit state function as a hyper-plane in multidimensional space, based upon the limit state value and its gradients in all directions. FORM works fine provided that the LSF is linear or near-linear in the region of interest. When the LSF is not linear enough, the higher order terms need to be included in the Taylor expansion in order to achieve better approximation of LSF. In SORM, second order terms are taken into account so that curvature of LSF is captured providing far better representation of LSF.

Kim and Yang (1997) calculated the probability failure of simple one dimensional spring-mass system under the assumption that both the excitation and system parameters are randomly distributed stochastic variables. Lee and Kim (2007) applied first- and second-order reliability method to estimate the failure probability of a crack in single edge crack specimen. They applied FORM, SORM and Monte Carlo simulation combined with Paris–Walker crack propagation model to estimate the failure probability of specimen under fatigue loading and concluded that the slope of Paris equation had the main influence on the failure probability. Yu et al. (2012) proposed an improved probabilistic fracture mechanics assessment method and modified sensitivity analysis to calculate the failure probability of high pressure pipe containing an semi-elliptical surface crack. They claimed that both methods can give consistent sensitivities of input parameters but the interval sensitivity analysis is computationally more efficient. Feng et al. (2012) analyzed the fatigue reliability of a stiffened panel subjected to the growth of correlated cracks. They applied both Monte Carlo simulation and FORM to estimate the failure probability, where the residual strength of the plate and stiffener in the stiffened panel was measured using crack tip opening displacement. Jensen (2015) suggests the use of FORM to get a better estimation of the tail in the distribution of the estimated fatigue damage and thereby reducing the variance. He considered the stresses in a tendon of TLP holding a wind turbine and found that the scatter of fatigue damage was reduced by a factor of three.

This paper extends the authors' previous work (Kang et al., 2015), where the flaw assessment following BS7910 was performed for a crack of a mooring anchor pile in a deterministic way. A semi-elliptical surface flaw in a weld toe of a mooring anchor pile subjected to both extreme and repeated fatigue loadings was assessed using FORM and SORM, and the failure probability was calculated under probabilistic crack length and depth. The LSF which corresponds to both static yield and fracture was approximated in joint probability space using first- and second-order method. The obtained failure probability was also compared with Monte Carlo simulation results which were obtained by running the sensitivity analysis module of RESCEW (Kang et al., 2015). Same analysis has been done for the LSF of fatigue, where a given loading spectrum was used as functional loading. For the LSF of fatigue, crack propagation analysis by numerically integrating Paris equation was performed based upon the procedure defined in BS7910.

2. Theoretical background

2.1. Flaw assessment procedure of BS7910

Flaw assessment procedure may be categorized into three different kinds, and they are fracture/yield assessment, fatigue assessment and combined fatigue-fracture/yield assessment. Because actual crack shape and stresses acting on it, together with material behavior, are too much complicated, the idealization on the analysis parameters is inevitable. Among others, the simplification and clarification on stresses are of utmost importance. Stresses acting on the flaw are classified into two kinds depending on its mechanical characteristics, such as primary and secondary ones. Primary stresses are defined as the stresses which may lead to the gross yield of net section, whereas the secondary stresses as those are not related to the yield of cross section. Stress on the wall of pressure vessel induced by the internal pressure is typical example of primary stress and residual stresses across the plate thickness are that of the secondary stress. Secondary stresses are not considered as a fatigue loading, but considered as a fracture/yield loading. On the other hand, stresses acting on flaws distribute quite complicated especially when the flaws are near the structural discontinuity, which is usually the case. This complicated stress field is processed in such a way that both membrane and bending components are extracted based on the stress linearization procedure and used for the flaw assessment.

Fig. 1(a) illustrates the fracture/yield assessment procedure, where a status was checked from static fracture as well as yield point of view. Some static loadings acting on a given geometry was analyzed and compared with both fracture toughness and yield strength of the material of interest. Depending on the consideration of combined effect of fracture and yield, three different Failure Assessment Diagrams (FAD) are proposed. Higher level of FAD is less conservative but it requests far more detailed information on the material behavior.

Fig. 1(b) summarizes fatigue assessment procedure. Dynamic stress, which may be represented by a given stress spectrum, acts on a specified initial crack of a geometry and the growth of crack with respect to the number of stress cycles is calculated by numerically integrating Paris equation. As was

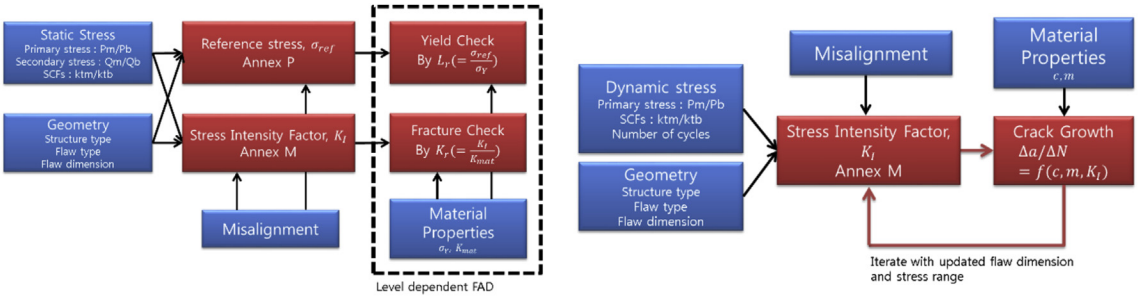

(a) Fracture/yield assessment (b) Fatigue assessment

Fig. 1. Fracture/yield and fatigue assessment procedure.

mentioned before, only primary stresses are considered in fatigue assessment. Fig. 2 shows combined fatigue-fracture/yield assessment procedure, where fracture/yield check is performed after every crack propagation step. Static stresses are used for periodic fracture/yield check and dynamic stresses are used for crack propagation.

Automatic flaw assessment program, RESCEW, based on the procedure specified in BS7910 was developed by Kang et al.(2015) as shown in Fig. 3. Unlike existing flaw assessment program, RESCEW contains some useful user friendly functions such as the criticality and sensitivity analysis of fatigue and fatigue-fracture/yield assessment, so that engineers can easily obtain flaw assessment results without time consuming repetition of calculation. All numerical calculations performed in this paper were done by RESCEW.

2.2. Limit state function

The limit state function in BS7910 is defined as so called FAD, which may further be categorized into level I, II and III depending on the conservatism that the assessment procedure has. The limit state function in BS7910 is defined as Eq. (1).

$$G = \left(1 - 0.14L_r^2\right)\left(0.3 + 0.7e^{-0.65L_r^6}\right) - K_r \tag{1}$$

where K_r and L_r mean fracture and yield ratio. K_r is the ratio of the stress intensity factor to the fracture toughness of the material and L_r is the ratio of reference stress to the material's yield stress. The variables that are supposed to be handled as random ones, e.g. crack length and depth, are melted in both K_r and L_r. K_r and L_r are defined as Eq. (2).

$$K_r = \frac{K_I}{K_{mat}}$$
$$L_r = \frac{\sigma_{ref}}{\sigma_Y} \tag{2}$$

where K_{mat} and σ_Y are the fracture toughness and material's yield stress respectively. The numerators K_I and σ_{ref} are the stress intensity factor and reference stress, which are defined as Eq. (3) for a semi-elliptical surface crack.

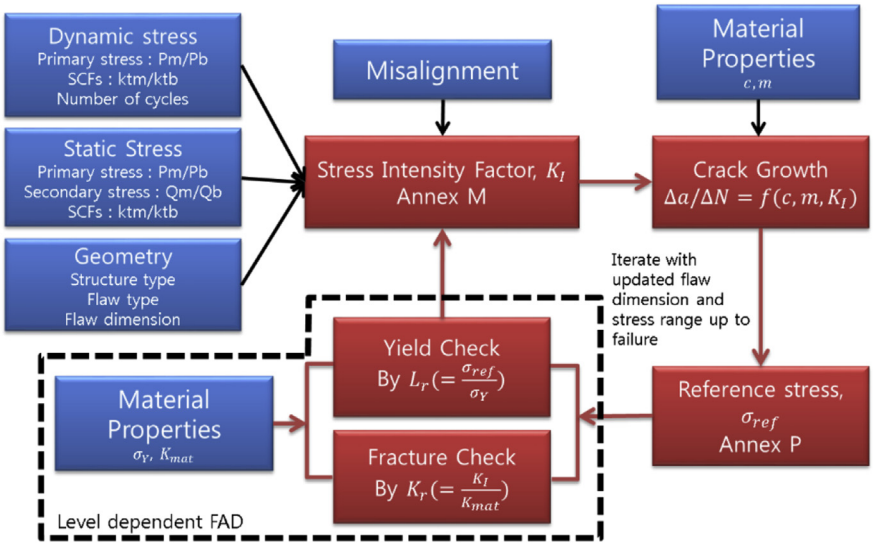

Fig. 2. Combined fatigue-fracture/yield assessment procedure.

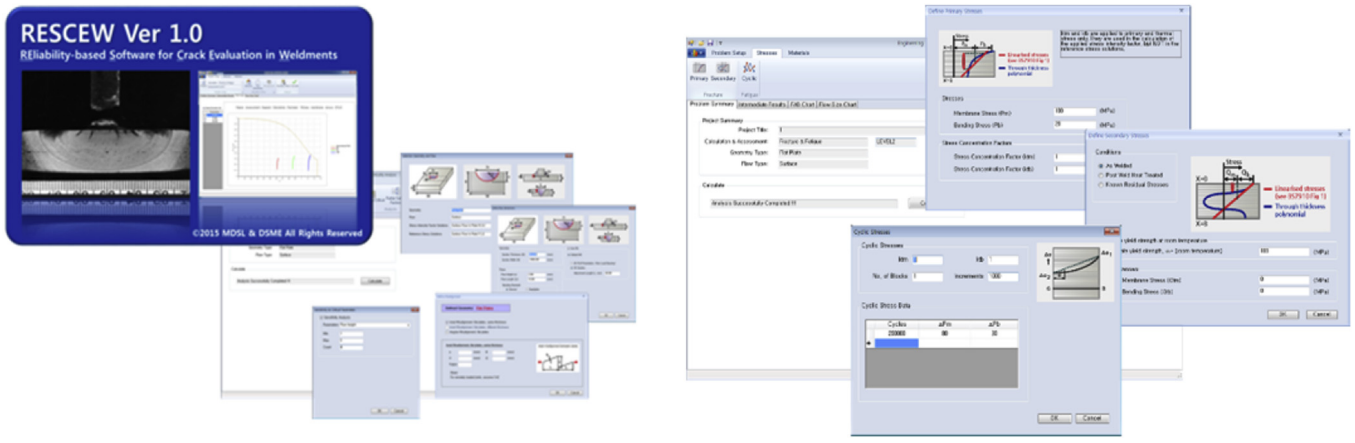

Fig. 3. RESCEW – Flaw assessment program (Kang et al., 2015).

$$K_I = (Y_{semi}\sigma)\sqrt{\pi a}$$

$$\sigma_{ref} = \frac{P_b + 3P_m\alpha'' + \left\{\left(P_b + 3P_m\alpha''\right)^2 + 9P_m^2\left(1-\alpha''\right)^2\right\}^{0.5}}{3\left(1-\alpha''\right)^2} \tag{3}$$

where Y_{semi} is a geometry function and α'' a correction factor to take into account the yield of uncracked area across the surface, which is given as a function of crack depth and length together with specimen size. If one assumes the probabilistic nature of both crack length and depth, both K_I and σ_{ref} become random variables as well, so that the Monte Carlo simulation may produces the points shown in Fig. 4(a). Fig. 4(b) shows bi-Gaussian type probabilistic distribution of two random variables X_1 and X_2, e.g. crack length and depth, along with the limit state function. The limit state function in X_1-X_2 space is generally unknown due to the complicated inter-relation between X_1-X_2 and $K_r - L_r$, and this complication become extreme when crack propagation is included in the flaw assessment.

Assuming that two random variables X_1 and X_2 follow Gaussian distribution and independent, as is represented by the scatted points in X_1-X_2 space of Fig. 4(b), the failure probability may be calculated by summing up the probability of the point that falls in the failure region, provided that the limit state function in X_1-X_2 space is known. The ultimate goal of this study is to approximate the unknown limit state function in X_1-X_2 space using the first- and second-order reliability methods described in the following section, so that one can calculate the failure probability without relying on the time consuming Monte Carlo simulation. Monte Carlo simulation takes long time especially when the fatigue crack propagation analysis is required because the computation has to be done for all possible combination of two variables. Moreover, once the number of variables increases, the computational burden increases exponentially, eventually leading to practically infeasible situation.

2.3. FORM and SORM

Assuming that two variables are supposed to be handled in probabilistic way, the limit state function is a curve in 2 dimensional random variable space and may be expressed by a line where the limit state surface becomes zero.

The limit state function is defined as Eq. (4), and is illustrated in Fig. 5, with the joint probability distribution of two random variables.

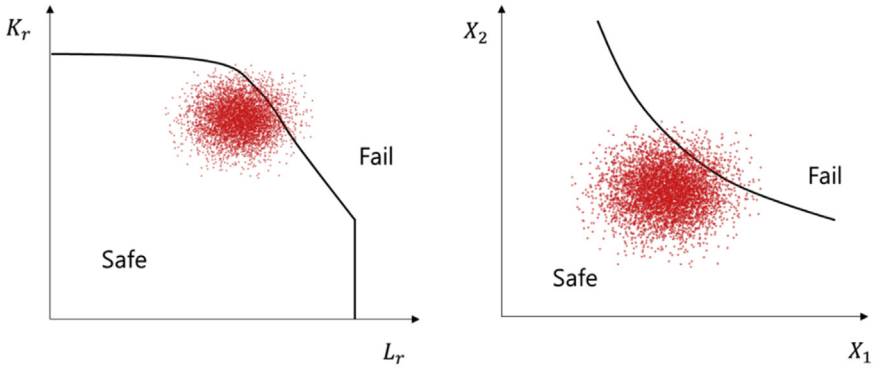

(a) LSF in K_r-L_r space (b) LSF in X_1-X_2 space

Fig. 4. Level 2 FAD (BS7910).

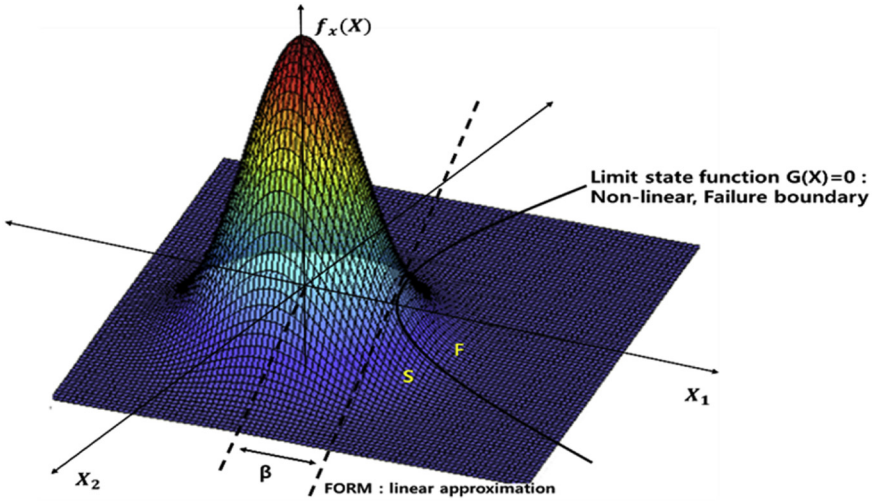

Fig. 5. Joint probability in X_1-X_2 space with LSF approximated by FORM.

$$G(X) = 0 \tag{4}$$

where X is a vector whose entries are random variables. In order to approximate the unknown limit state function, one may start with the Taylor series expansion of $G(X)$ with respect to the random variable vector X. Taylor series expansion of $G(X)$ up to second order with respect to the position X^* will lead to Eq. (5).

$$G(X) = G(X^*) + \nabla G(X^*)^T \cdot (X - X^*) + \frac{1}{2}(X - X^*)^T \cdot \nabla^2 G(X^*) \cdot (X - X^*) \tag{5}$$

where ∇ and ∇^2 means gradient and hessian operator. Approximation of the limit state function using FORM or SORM may be easily done with Eq. (5) provided that the design point denoted by X^* is given. However, this design point is not a priori known hence should be determined by iterative method.

1. Coordinate transform from physical to standardized space

$$u = \frac{X - \mu}{\sigma}$$

2. Start with arbitrarily chosen initial point u_0
3. Expand $H(u)$ using Taylor series based upon the derivatives at u_0

$$H(u) = H(u_0) + \nabla H(u_0)^T \cdot (u - u_0) + \frac{1}{2}(u - u_0)^T \cdot \nabla^2 H(u_0) \cdot (u - u_0)$$

4. Define the limit state function by $H_0(u) = 0$
5. Find the closest point on $H_0(u) = 0$ from the mean value, and set this point as u_1

$$\beta = min\|u\| \;\; subject\ to\ H_0(u) = 0$$

6. Go to step 2 for next iteration and repeat 2 to 5 until convergence is achieved

$$\beta_{i+1} - \beta_i < \varepsilon$$

The shortest distance between the limit state function and the origin of standard space, β, is defined as the reliability index, which is shown in Fig. 6. Once the random variables are standardized, with its mean and standard deviation, the closest possible point on the limit state function determines the failure probability, hence the larger the distance becomes, the less probable the failure becomes. Step 3 requires the calculation of limit state function at the current location together with both gradient vector and hessian matrix. For the calculation of gradient vector and hessian matrix, the finite difference scheme was employed. Therefore, RESCEW was called in total 6 time for the calculation of required 6 quantities in $H(u_0)$, $\nabla H(u_0)$ and $\nabla^2 H(u_0)$.

3. Application to mooring anchor pile

3.1. Analysis conditions

A target structure selected for the flaw assessment is a mooring anchor pile of FPSO, whose diameter within the parallel middle body is 5.5 m and the wall thickness is 100 mm. Dynamic load acting on the anchor pile, which is used for the fatigue assessment, is hammering load to force the pile to penetrate into the seabed, and it acts only in-plane axial direction. For static load, which is used for the fracture/yield assessment, the maximum load which the pile can experience during operating period of FPSO was taken into account. The welded joint of the anchor pile was made by butt welding and the semi-elliptical surface crack was assumed to be present at the toe of the weld. Two separate flaw assessments were performed in this study. One is fracture/yield assessment under the most probable extreme load acting on the anchor pile and the other one is combined fatigue-fracture/yield assessment

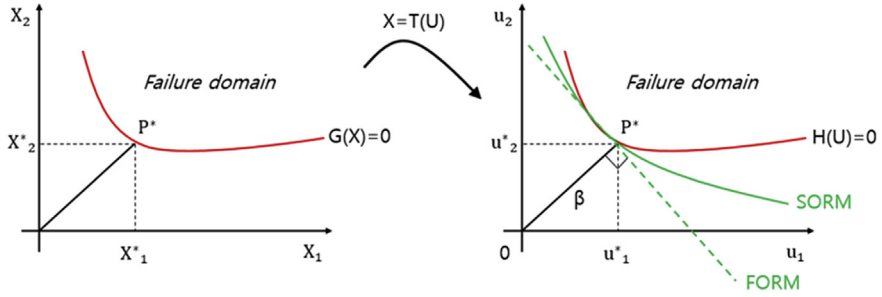

(a) Physical space (b) Standard space

Fig. 6. Definition of reliability index.

under repeated hammering load during the piling stage. Fig. 7 shows the shape of the mooring anchor pile having a weld defect.

Even though the base structure that contains the target crack is circular cylinder shape, the semi-elliptical surface crack on a flat plate was assumed in this analysis. This may be justified based on the fact that the final crack length and depth is relatively small compared to the diameter of the cylindrical shaped pile. The width of the flat plate was assumed to be arbitrarily large. The dimensions of the assumed target plate and flaw are as follows:

- Width(W): 10000 mm
- Thickness(B): 100 mm
- Length of flaw (2c): 11.5 mm
- Depth of flaw(a): 7 mm
- Length of welded connection(L): 85 mm

The length and depth of the semi-elliptical surface crack is based on the nondestructive test results actually carried out after the fabrication. Fig. 8(a) shows a snapshot of program input such as dimension of geometry, flaws and condition of welded joint.

It is well known that axial or angular misalignment of a welded joint introduces additional bending stress increasing the total stress range near the joint so it tends to have some negative impacts on the fatigue life. Therefore, the bending stress due to misalignment should be considered in calculating total stress range. The projected lengths, l_1, l_2 are 2000 mm, and the misaligned height, e and thickness of plate, B are 4 mm and 100 mm, respectively. Assuming that the joint is unrestrained, 6 was applied as the restraint factor according to BS7910. Fig. 8(a) shows program inputs for the axial misalignment.

For calculation of fatigue crack growth rate, Paris constants for flaws of welded steels recommended by BS7910 were used, and two stage crack growth relationship was applied. As shown in Table 1, 63 N/mm$^{3/2}$ for threshold stress intensity factor (ΔK_{th}) and 144 N/mm$^{3/2}$ for stage A/B transition point were used, respectively. Tables 1 and 2summarizes the Paris constants and other relevant material properties used in this analysis.

For the static fracture/yield assessment, the expected extreme load acting on the structure during its life time was used. The primary membrane stress was set to be 139 MPa and secondary membrane stress was set to be 414 MPa. The secondary membrane stress in this particular case corresponds to the residual stress, which was assumed to be the magnitude of the yield stress of the material. For both cases, the bending stress was assumed to be absent. Fig. 9 shows the dynamic stress spectrum used for the crack propagation analysis. These are the values provided by the anchor pile manufacturer.

In this study, both crack length (2c) and depth(a) of semi-elliptical surface crack at weld toe were handled as random variables whose probability distribution was defined as Gaussian with given means and standard deviations as shown in Table 3. The mean values was chosen as the reported measured value and the standard deviation was assumed to be 1 mm. The joint probability was defined as the product of the two Gaussian distribution under the assumption that two variables are independent with each other.

In this analysis, a fracture/yield assessment and a combined fatigue-fracture/yield assessment have been carried out in both deterministic and probabilistic ways, respectively. First, the deterministic approach was taken to check the acceptability of the existing flaw from both static and dynamic point of view. This calculation precisely matches the recommendation of BS7910, so that one can eventually see whether the flaw is acceptable or not. Then, the reliability based analysis was performed using FORM, SORM. Monte Carlo simulation was also performed to check the validity of the analysis results obtained by FORM and SORM. While doing Monte Carlo

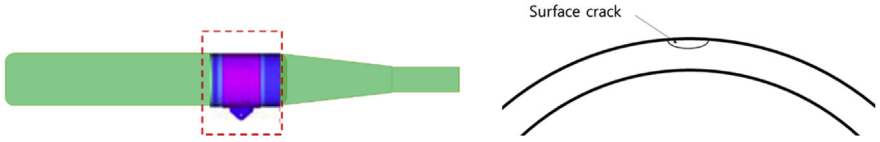

Fig. 7. Mooring anchor pile and surface crack.

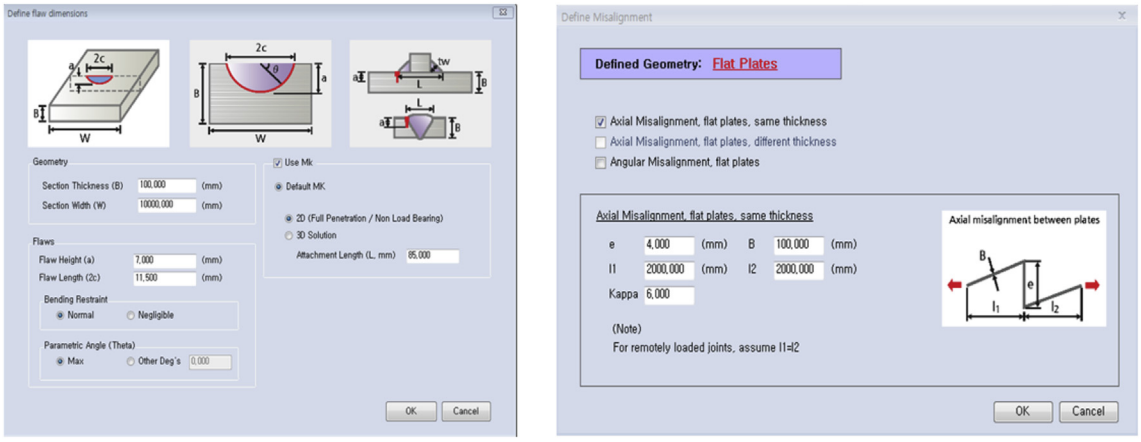

(a) Flaw type and dimension (b) Axial misalignment

Fig. 8. RESCEW input.

Table 1
Paris constants.

Material	A	m	ΔK [N/mm$^{3/2}$]
Steel, including austenitic	2.1e-17	5.1	63
	1.29e-12	2.88	144

simulation, the sensitivity module of RESCEW was employed to minimize the user interruption required for the repetitive calculation.

3.2. Fracture/yield assessment

A fracture/yield assessment has been carried out for an initial flaw under static load. Analysis conditions explained in 3.1 were applied, and a deterministic flaw assessment was performed. Fig. 10 shows the result of the deterministic fracture/yield assessment using FAD. As a result of the analysis, $K_r = 0.831$ and $L = 0.348$ were obtained as fracture ratio and yield ratio, respectively so it can be concluded that the initial flaw is acceptable under the given static load since the assessment point falls inside the safe region of Level II FAD.

Prior to the FORM and SORM analysis, Monte Carlo simulation was carried out under static load so that one can

Table 2
Material properties.

Yield strength [MPa]	Tensile strength [MPa]	Young's modulus [MPa]	Poisson ratio	CTOD [mm]
414	517	2.06e5	0.3	0.2

Cycles	$\Delta\sigma_m$ [MPa]	$\Delta\sigma_b$ [MPa]
265.5	275	0
796.5	250	0
265.5	200	0
265.5	175	0
265.5	150	0
796.5	125	0
1858.5	100	0
11151	50	0
79915	25	0

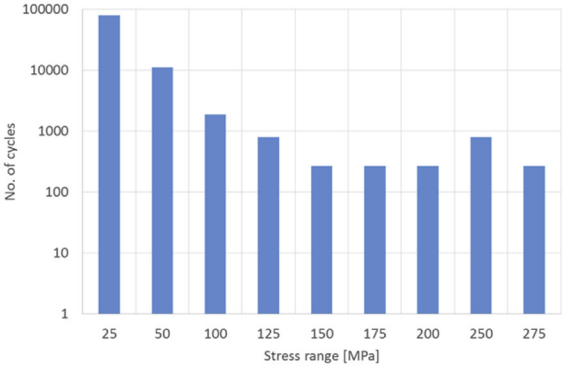

Fig. 9. Dynamic stress spectrum.

Table 3
Assumed probability parameters of crack length and depth.

Parameter	Mean [mm]	Standard deviation [mm]
Flaw length (2c)	11.5	1
Flaw depth (a)	7	1

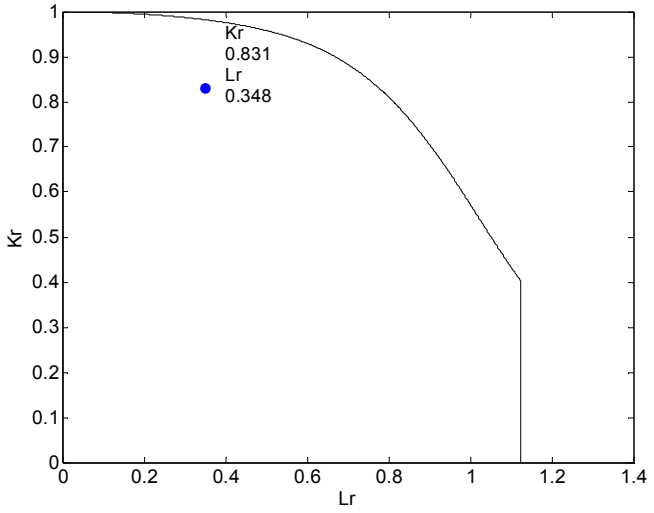

Fig. 10. Deterministic fracture/yield assessment result.

obtain the true limit state function. For the Monte Carlo simulation, all possible combinations of crack length and depth were explored and the true limit state function was calculated based upon Eq. (1). Fig. 11(a) shows the true limit state surface which is calculated by the sensitivity module of RESCEW. The region of positive contour value means the crack is safe and the one of negative contour value unsafe. Upper left area where the contour is not defined is the area within which the combination of crack length and depth is not practically feasible. A curve which define $G(X) = 0$ is the true limit state function, which is illustrated with joint PDF in Fig. 11(b). In this particular Monte Carlo simulation, both crack length and depth are sampled with the interval of 1 mm, within the range of 1 mm−80 mm, eventually leading to 3200 simulation cases. The failure probability was calculated by adding up the probability of the points that lie within the failure region, as shown in Fig. 11(b). The resulting failure probability was 8.29-e-4%.

The true limit state function and resulting failure probability was estimated by FORM and SORM. As was stated before, the design point which the first- and second-order approximation were made at should be determined in iterative way until the convergence is achieved. During the calculation process of FORM and SORM, both gradient and hessian of the limit state function should be evaluated at every iteration step.

Fig. 12 shows the evolution of approximated limit state function by first- and second-order method. The red marks in Fig. 12 indicate the interim design points and this tends to converge to the ultimate design point. It can be clearly seen that the second-order method converges much quicker than the first-order method, as expected.

Fig. 13 shows true and approximate limit state function together with joint PDF of crack length and depth. Fig. 13 demonstrates the fact that FORM approximates the true limit state function fairly well, and SORM in almost perfect way. The calculated failure probability using FORM and SORM are 8.52e-4% and 8.29e-4%,which give rise to 2.8 and 0% error, respectively.

3.3. Combined fatigue-fracture/yield assessment

A combined fatigue-fracture/yield assessment was performed for a given initial flaw. The difference between fatigue-fracture/yield assessment from fracture/yield assessment lies on the fact that the former one requires the crack propagation analysis, hence the computational burden for Monte Carlo simulation is much larger. For the crack propagation analysis, the well-known Paris equation was numerically integrated using 4th order Runge-Kutta method. The stress spectrum was arranged in descending order, which is known to produce the most conservative result, and applied in repetitive way after dividing it into several blocks. Fig. 14 shows analysis results of deterministic fatigue-fracture/yield assessment results. Fig. 14(a) indicates that the crack length and depth increase as the number of cycles, which was represented by a fracture of total life in the horizontal axis, increases. In fatigue-fracture/yield assessment, the static fracture/yield is assessed

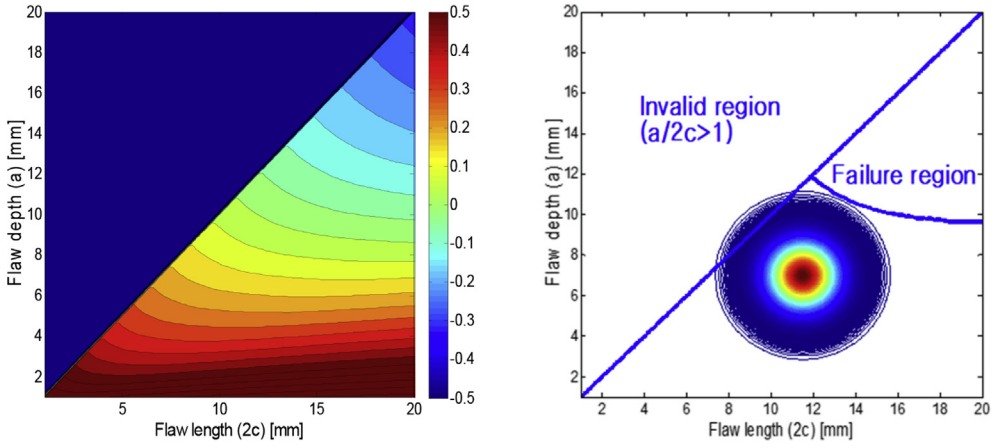

(a) Limit state surface

(b) Limit state function and joint PDF

Fig. 11. Monte Carlo simulation results of fracture/yield assessment.

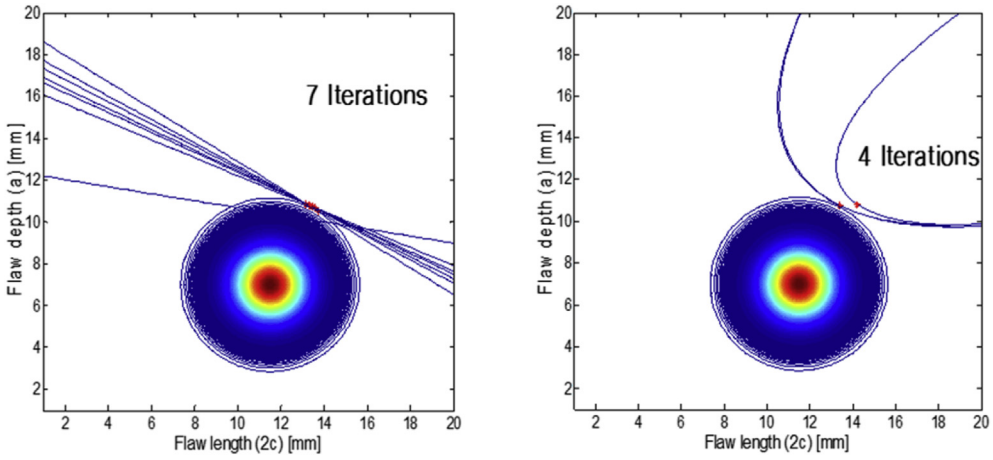

(a) FORM (b) SORM

Fig. 12. Convergence of approximated limit state function for fracture/yield assessment.

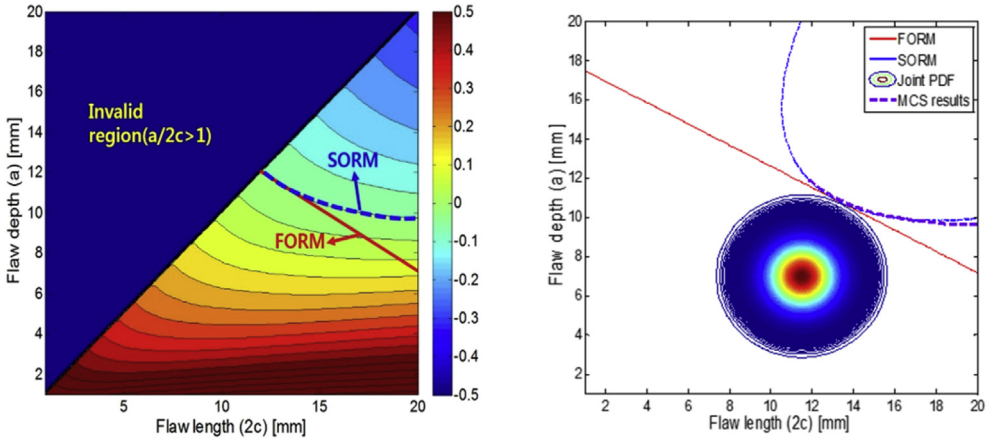

(a) Limit state surface and FORM/SORM (b) True and approximated LSF with joint PDF

Fig. 13. Reliability analysis results for fracture/yield assessment.

periodically with a certain interval of fatigue loading cycles, hence produces series of points in FAD as shown in Fig. 14(b). Fig. 14(b) shows that the final crack size, measured at the end of the fatigue loading cycles, still stays within the safe region of FAD, even though it almost reached the borderline. The final crack depth was 11.5 mm, and length 85.17 mm. Judging from the close distance from the final assessment point to the horizontal part of FAD, one may conclude that it is more likely for the crack to be fractured if additional number of cycles is applied to the structure.

Again, Monte Carlo simulation for the combined fatigue-fracture/yield assessment was performed with the combinations of initial crack length and depth. Fig. 15(a) shows true limit state surface obtained from Monte Carlo simulation. Limit state surface shown in Fig. 15(a) was obtained based on the Eq. (1) after the entire crack propagation analysis was completed. It is noteworthy that this limit state surface corresponds to that of the final crack size, but the crack length and depth of horizontal and vertical axis of the graph is that of initial crack. Similar to the case of fracture/yield assessment, the region of positive contour value means the crack is safe and the one of negative contour value unsafe. A curve which define $G(X) = 0$ is the true limit state function, which is illustrated with joint PDF in Fig. 15(b). It is natural to expect that the limit state function is located far lower than what has been observed in case of fracture/yield, because of additional fatigue loading which enlarged the crack size by large amount. The calculated failure probability in this particular example turned out to be 35% (see Fig. 16).

Fig. 17 shows true and approximate limit state function together with joint PDF of crack length and depth. Fig. 17 clearly demonstrates that both FORM and SORM

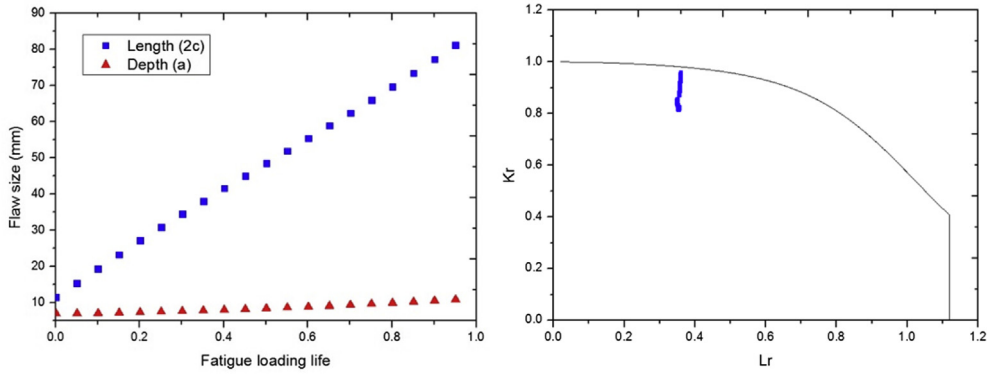

(a) Crack growth curve for depth and length (b) FAD during crack propagation

Fig. 14. Deterministic fatigue-fracture/yield assessment results.

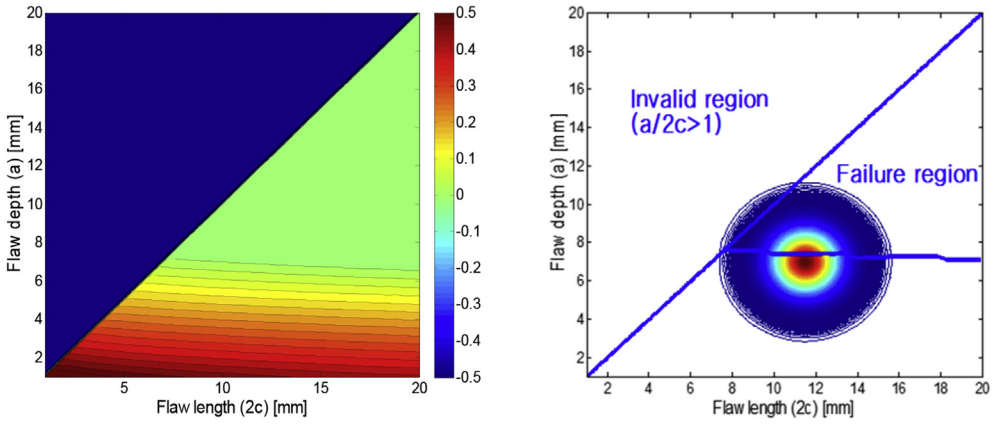

(a) Limit state surface (b) Limit state function and joint PDF

Fig. 15. Monte Carlo simulation results of fatigue-fracture/yield assessment.

approximate the true limit state function fairly well. The performance of FORM is better in this case since the true limit state function is less curved. The calculated failure probability using FORM and SORM are 37% and 36%, which is very close to the true value.

4. Conclusions

In this study, efforts have been made to develop a reliability-based flaw assessment procedure using the first- and second-order reliability method, which is in line with the procedure of BS7910. Based on the study results described so far, following conclusions are derived.

- A reliability-based flaw assessment procedure, combined with BS7910 was developed and successfully applied to the mooring anchor pile example. The validity of the procedure was confirmed based upon the comparison with Monte Carlo simulation results.
- FORM-based approximate limit state function was sought using the first order multi-dimensional Taylor series expansion. The design point was successfully found by iterative procedure until the convergence was achieved. It was found that the FORM-based limit state function captures the true limit state function with acceptably good accuracy.
- SORM-based approximate limit state function was sought using the second order multi-dimensional Taylor series expansion. In this case, numerically more expensive Hessian matrix should be evaluated at every iteration step so that the computational cost increases compared to the FORM. The accuracy of SORM-based limit state function turned out to be far better than that of FORM.
- The methodology has been applied to the mooring anchor pile problem, for both fracture/yield and fatigue-fracture/yield assessment point of view. As to the fracture/yield assessment, the failure probability obtained from FORM and SORM was 8.52e-4% and 8.29e-4%, which are close to 8.29-e−4% of Monte Carlo simulation.
- For the fatigue-fracture/yield assessment, the failure probability calculated by FORM and SORM was 37% and 36% respectively. The approximate results are very close to the result of Monte Carlo simulation, which was 35%.

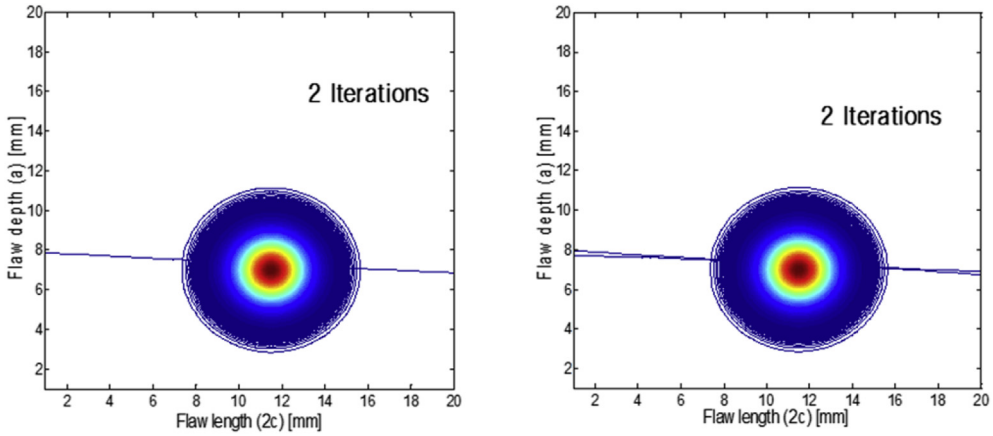

(a) FORM (b) SORM

Fig. 16. Convergence of approximated limit state function for fracture/yield assessment.

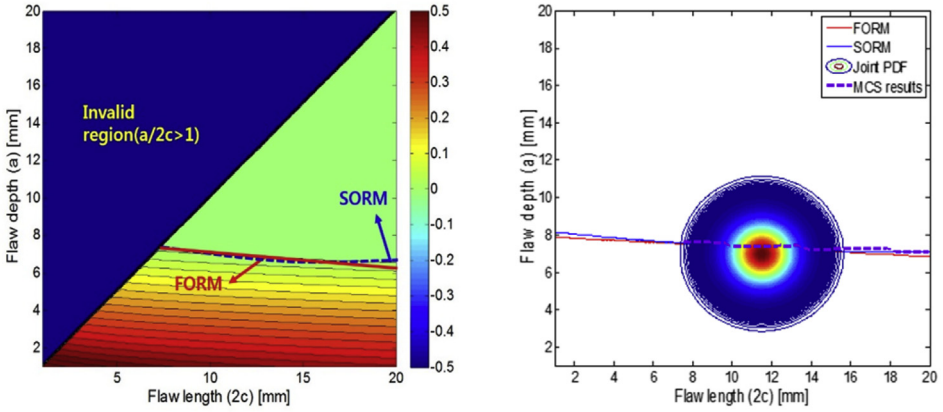

(a) Limit state surface and FORM/SORM (b) True and approximated LSF with joint PDF

Fig. 17. Reliability analysis results for fatigue-fracture/yield assessment.

Acknowledgement

This study was supported by a Special Education Program for Offshore Plant by the Ministry of Trade, Industry and Energy Affairs (MOTIE). This research was also financially supported by Korea Evaluation Institute of Industrial Technology (KEIT, Korea) and the Ministry of Trade, Industry & Energy (MOTIE, Korea) through the core technology development program of Industrial Convergence Technology (10045212, Predictive maintenance system for the integrated and intelligent operation of offshore plant).

References

American Petroleum Institute(API), 2007. Fitness-for-service, API 579–1/ASME FFS-1.

Breitung, K., 1984. Asymptotic approximations for multinormal integrals. J. Eng. Mech. 110 (3), 357–366.

British Standard Institution(BSI), 2005. Guide to Methods for Assessing the Acceptability of Flaws in Metallic Structures, p. BS7910.

Cornell, C.A., 1969. A probability-based structural code. J. Am. Concr. Inst. 66 (12), 974–985.

Feng, G.Q., Garbatov, Y., Guedes Soares, C., 2012. Fatigue reliability of a stiffened panel subjected to correlated crack growth. Struct. Saf. 36–37, 39–46.

Fiessler, B., Neumann, H.J., Rackwitz, R., 1979. Quadratic limit states in structural reliability. J. Eng. Mech. 105 (4), 661–676.

Hasofer, A.M., Niels, C., Lind, A.M., 1974. Exact and invariant second-moment code format. J. Eng. Mech. 100 (1), 111–121.

Hohenbichler, M., Gollwitzer, S., Kruse, W., Rackwitz, R., 1987. New light on first- and second-order reliability methods. Struct. Saf. 4, 267–284.

Jensen, J.J., 2015. Fatigue damage estimation in non-linear systems using a combination of Monte Carlo simulation and the first order reliability method. Mar. Struct. 44, 203–210.

Kang, B.J., Kim, Y., Ryu, C.H., Park, S.G., Oh, Y.T., 2015. Flaw assessment on an offshore structure using engineering criticality analysis. J. Soc. Nav. Archit. Korea 52 (6), 435–443.

Kim, I.H., Yang, Y.S., 1997. Structural reliability analysis of linear dynamic systems with random properties. J. Soc. Nav. Archit. Korea 34 (4), 91–98.

Lee, O.S., Kim, D.H., 2007. Reliability of fatigue damaged structure using FORM, SORM and fatigue model. In: Proceedings of the World Congress on Engineering, London, UK.

Metropolis, N., Ulam, S., 1949. The Monte Carlo method. J. Am. Stat. Assoc. 44 (247), 335–341.

Rackwitz, R., Fiessler, B., 1978. Structural reliability under combined random load sequences. Comput. Struct. 9 (5), 489–494.

Tvedt, L., 1990. Distribution of quadratic forms in normal space – application to structural reliability. J. Eng. Mech. 116 (6), 1183–1197.

Yu, Z., Zheng, Z., Qunpeng, Z., 2012. Improved reliability analysis method based on the failure assessment diagram. Chin. J. Mech. Eng. 25 (4), 832–837.